Journal of
Mechanical
Science and
Technology

Journal of Mechanical Science and Technology 21 (2007) 1892~1900

Numerical and experimental studies of thin liquid film flow between two forward-rollers

Chia-Hung Chien and Jiin-Yuh Jang*

Department of Mechanical Engineering,
National Cheng-Kung University Tainan, 70101, Taiwan

(Manuscript Received May 7, 2007; Revised August 7, 2007; Accepted August 7, 2007)

Abstract

Roll coating is a widely used industrial technique to deposit a thin and uniform liquid film on a sheet or solid substrate.In this paper the three dimensional forward roll coating process has been studied by both experiments and numerical simulations. Experiments were conducted on a 2 roll coating system of pick up roll and application roll using two samples of 50% and 70% by weight aqueous glycerin solutions. The gap between the two rollers at nip was maintained at 100 microns. The coating film thickness and the distance of the film splitting point from the nip were measured during the experiments. The coating film thickness was determined for different speed ratios for both samples. 3D Numerical simulations for forward coating process have been carried out and the simulation results were verified were with experiments. They match very well, the error between them being 5% to 10%.

Keywords: Forward-roller; Coating; CFD

1. Introduction

Currently, coating technology is widely used in many industrial applications such as rubber tape, film, tape, electronic parts, recorders, and electronic products. Among various coating methods, roll coating is a simple and convenient means for depositing a thin liquid film on a moving substrate. Generally, two or three or sometimes more cylindrical rolls are combined to produce a coating film of desired thickness in practice. According to the direction of rotation between the two rolls, the roll coating process can be divided into forward roll coating and reverse roll coating. The process is called 'forward roll coating' if the two rolls are moving in the same direction. On the other hand, if the two rolls are moving in opposite directions in the nip region, the process is termed as 'reverse roll coating'. Among the two, forward roll coating is most commonly used to produce high quality, ultra thin coating films of low viscosity liquids [1].

During the forward roll coating process, the fluid flow is two dimensional and is steady at low speeds. As the roll speed increases, the two dimensional flow becomes unstable and the thin-coated film surface will not be smooth but will be covered by either regular or irregular patterns or strips of hydrodynamic origin. This type of flow instability of liquid, or rather the three-dimensional flow to which it may lead, is commonly called 'ribbing'. The ribbing affects the quality of finished product of the roll coating process. Therefore, the fluid flow analysis of roll coating is essential and is a basic necessary step during the design stage of the roll coating process.

Over the last few decades, many extensive investigations have been carried out on forward roll coating process to study the film-splitting flow of coating fluid and associated instability. Most of the early works on forward roll coating used hydro-

*Corresponding author. Tel.: +886 6208 8573, Fax.: +886 6234 2232
E-mail address: jangjin@mail.ncku.edu.tw

dynamic lubrication theory ignoring the effect of surface tension. Subsequent research used an approximate solution of Navier–Stokes equations using numerical methods like finite volume method (FVM) and finite element method (FEM).

Pearson [2] was the first to analyze the forward roll coating process to show why in many cases flow leading to a uniform film is unstable. He was able to account for the appearance of regularly spaced crests and troughs in the emergent thin film running parallel to the direction of motion of the spreader. Further theoretical and experimental studies were carried out by researchers [3-7] to describe the film-splitting instability between rigid rolls based lubrication theory of hydrodynamics. Coyle et al. [8] analyzed the liquid flow in a narrow gap between two rotating cylinders of forward roll coating. They predicted and showed through their experiments that the ratio of the film thicknesses on the two rolls equaled the speed ratio to the 0.65 power. The Galerkin finite-element solutions gave full details of the steady two-dimensional free-surface flows including complex recirculation patterns in the film-splitting region and showed how the film splitting stagnation line became a static contact line in the limit as one roll surface becomes stationary. Coyle et al. [9] investigated the ribbing instability both theoretically and experimentally in forward roll coating. The Navier-Stokes system of equations for the two-dimensional flow in symmetric film-splitting was solved by FEM. They also examined the stability of the flow with respect to three-dimensional disturbances by applying linear stability theory. Hasegawa and Sorimachi [10] made an experiment on ribbing induced on a film coated over a roll surface by a two-roll system in which one roll was rotated with a speed and the other fixed or rotated with relatively different speeds. Wavelength and depth of ribbing were measured by a technique that utilizes an image of a straight bar placed above the roll and reflected on the ribbing film surface.

Gurfinkel and Patera [11] proposed a framework for interpreting the formation, evolution, spatial persistence of ribbing and parallel spectral element simulations of the full unsteady three-dimensional nonlinear free-surface fluid flows during the coating process. The framework couples, by means of a transition region, the 'viscous fingering' instability of a splitting meniscus and the leveling of viscous films under the effect of surface tension. However the drawback of their approach was a stability restriction on the maximum allowable time step since they treated the domain evolution explicitly.

Carvalho and Scriven [12] used a linear, three-dimensional stability analysis of free surface flows to study the instability that arises in film-splitting flows between counter-rotating rolls in a deformable gap. They indicated how a deformable cover could be used to delay the onset of ribbing in forward-roll coating and deformable gaps could be operated at higher speeds without producing non-uniform profiles in the cross-web direction.

It is clear from the above literature that most of the investigations used 2D flow analysis and simplified theory for 3D flow analysis to study the complex ribbing process in forward roll coating. The predictions cannot be expected to be accurate over the entire range of parameters for which observations have been published. This motivated the present investigation for accurate analysis of 3D forward roll coating process considering full Navier Stokes equations. In this study, the flow governing equations are solved by finite volume method through the use of commercial software code. The experiments were conducted by using glycerin-water solutions. The effect of roll speed on film thickness and the location of fluid film splitting point with respect to roll speed have been investigated by experimental simulations.

2. Mathematical analysis

The simple roll coater used in the forward roll coating process is shown in Fig. 1. The two rolls rotate in opposite directions and move with the same or different peripheral speeds. The two rolls are called "pick up roll" and "application roll." Liquid to be coated is picked up from a coating bath or enamel pan

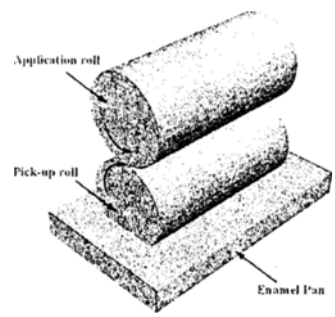

Fig. 1. Pictorial view of a two-roll forward roll coater.

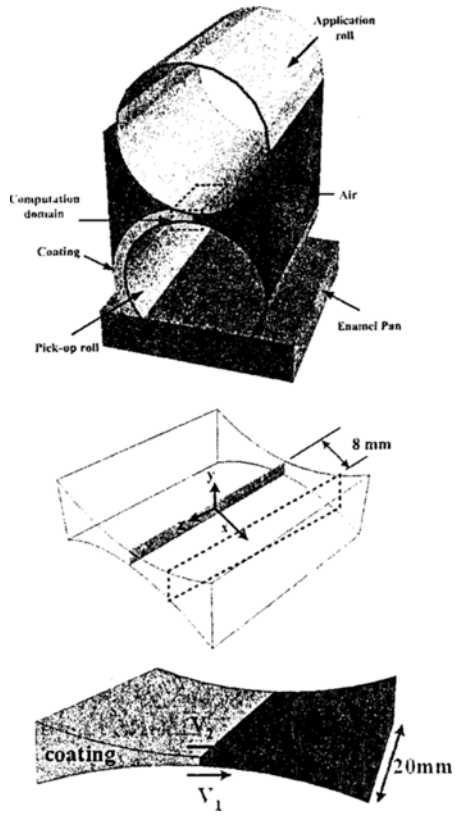

Fig. 2. Computation domain at the nip region.

by the action of viscous lifting. The computational domain is shown in Fig. 2. The fluid flow is assumed to be an incompressible and isothermal laminar flow. The system of flow 3-D governing equations may be expressed in the form

$$\nabla \cdot \vec{u} = 0 \tag{1}$$

$$\rho \frac{\partial \vec{u}}{\partial \tau} + \rho(\vec{u} \cdot \nabla)\vec{u} = \rho \vec{g} - \nabla P + \mu \nabla^2 \vec{u} \tag{2}$$

The coating fluid and the air are considered as two separate fluids in the forward roll coating process and the interface between them is predicted by using fluid front tracking algorithms. The volume of fluid (VOF) technique is widely used among the available tracking algorithms since it gives comparatively very accurate results. Hence in this study the VOF method [13] is used to determine the free surface location or the interface between the coating fluid and the air.

The free-surface location is determined via solution of the following equation:

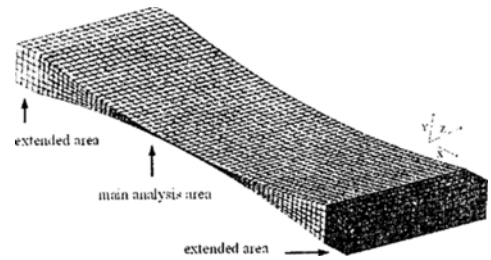

Fig. 3. Finite volume grid for simulation.

$$\frac{\partial F}{\partial \tau} + F(\nabla \cdot \vec{u}) = 0 \tag{3}$$

This VOF method allows us to set up a special parameter F (the volume fraction) for Eq. (3) applied at the interface between air and coating. When F is one, it represents that only coating is included. When F is zero, it represents that it only includes air. The range of F is between zero and one.

At the inlet and outlet area, the pressure was fixed at 1 atm, the liquid volume fraction F was assumed to be 1 and 0, respectively. At the solid surfaces, no-slip conditions for the velocity are specified (v_1=30 m/min and v_2= 30~120 m/min). On both ends of the z axis for the computational domain, the cyclic boundary conditions were assumed. At the interface between air and glycerin solution, one has

$$n \cdot \overline{\overline{T}} = \frac{1}{Ca} \frac{dt}{ds} - n\, p_a \tag{4}$$

Here $\overline{\overline{T}}$ is the stress tensor in fluid, n and t are the unit vectors normal and tangential to the boundary surfaces, respectively. s is the arc length along the free surface and dt/ds is the curvature of the free surface. Pa is the ambient pressure and Ca, the capillary number, is defined as the ratio of viscous force to surface tension forces.

3. Numerical analysis

Numerical simulations were carried out by using a commercial CFD software package CFD-RC [14] which uses finite volume method to solve the governing equations. The two rolls of forward roll coater have a roll radius of 15cm and the gap between the rollers is 100 micron. A mixture of water and the glycerin is used as coating fluid. The modeling of the problem has been done with CFD-GEOM software. The grid is generated by using structural 3-D block

elements. The finite volume grid is shown in Fig. 3. The basic fluid flow and VOF models are used in CFD-AC+ solver to simulate the fluid flow at the nip region between the two rolls.

The simulations were performed on a workstation with Intel Xeon 3.4 + 3.4 GHz CPU, and typical CPU times were 12 hours. The simulation results are verified by the experimental results by conducting a series of experiments for thin film coating using a 2 roll forward roll coater under identical conditions to that considered in the numerical simulation. The numerical results are in good agreement with experimental results, error being 5%. The measured coating film thickness and the location of the film splitting point from the nip point almost matches that obtained from numerical simulation.

4. Experimental set-up

Experiments were conducted on a two-roll forward roll coating machine depicted in Fig. 4. The coating machine consisted of two horizontally mounted, equal diameter, polished, hard chrome plated steel rolls driven by two separate motors with feed back control system. The rolls were of 150 mm radius each and of 300 mm length. Gap between the two rolls was of the order of magnitude of 100μm (4 mils). The high-speed production roll coating machine consists of three motors. One of them was connected to the pick-up roll to give a maximum rotation speed of 85m/min and the other connected to the application-roll provided the maximum speed of 275 m/min. The application roll was made to rotate at different speeds while the pick-up roll was kept at a predetermined speed. The pick-up roll was maintained at 30 m/min and the applicator roll speed was varied as 30, 60 and 120 m/min for different cases. Aqueous glycerin containing a solution of glycerin and water was used as the coating fluid. The enamel pan or coating fluid reservoir was filled with a pre-measured quantity of aqueous glycerin solution. The pick-up roll was partially immersed in the enamel pan. When the pick-up roll starts rotating, it automatically picks the coating fluid and carried away along the surface. The coating fluid enters at the nip region and then splits into two portions, one being followed along the applicator roll surface and the other along the pick-up roll surface. During this process the applicator roll became coated with coating fluid and the coating fluid along the pick-up roll was returned to the enamel pan. Experiments were conducted for two different aqueous glycerin solutions which contained 50% and 70% by weight glycerin. The viscosity of the coating fluid was 4.99cP and 19.58cP for 50% and 70% by wt. glycerin solution. The measurement system used to measure the film thickness, shown in Fig. 5, uses an electronic micrometer-driven needle which directly measures the coating thickness. Initial reading was noted by setting the calibrated micrometer on the roll surface such that the needle just touched the roll surface. When measuring the thickness of the coating film, one waits until the coating is uniformly applied on the application roll surface. Again the micrometer reading directly gave the film thickness. The procedure was repeated three more times and the average of the best three readings was taken as the film thickness value and hence the error in measurement was minimized. Experiments were conducted for 50% and 70 % aqueous glycerin solutions for different speeds of applicator roll to achieve a speed ratio of 1,2 and 4 while the pick-up roll speed was kept at 30 m/min. Coating film thickness was measured for each set of experiments,

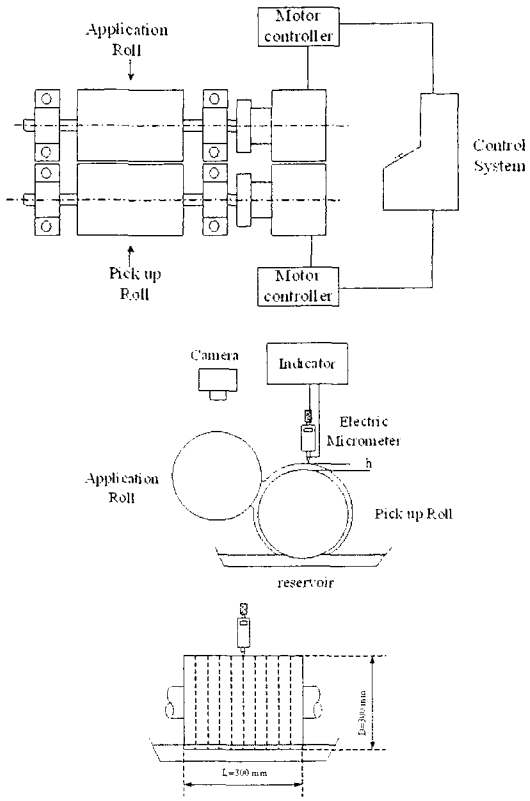

Fig. 4. Experimental machine with feedback control system.

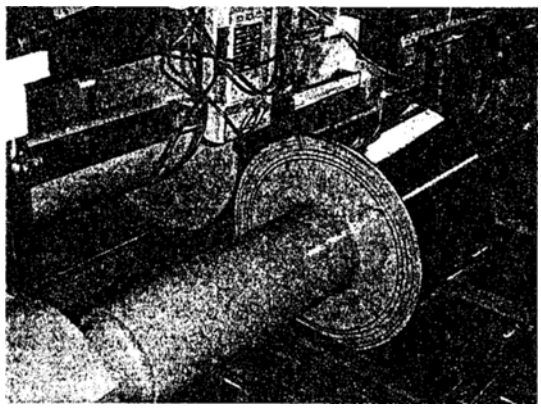

Fig. 5. Film thickness measurement system.

and also the ribbing occurrence phenomenon was closely observed during the experiments, especially at high speeds.

5. Result and discussion

The numerical simulations and experiments were conducted for two different samples of aqueous glycerin solution as a coating fluid, one with 50% by weight of glycerin and other with 70% by weight of glycerin. Post-processing of numerical results was carried out by using CFD-View tool of CFD-RC software. In all numerical simulations and experiments the gap distance between the two rolls was maintained at 100 microns. A typical grid system of 201 x 14 x 21 grid points was adopted in the numerical computations. A careful check for the grid-independence of the numerical solutions was made to ensure the accuracy of numerical results. For this purpose, four grid systems, 101x7x11, 201x14x21, 301x21x31 and 401 x 14 x 21, were tested. It was found with the 201x14x21 grid system that for a speed ratio of 1, the relative errors for the coating film thickness values were less than 5% for the latter three grid systems. The coarse grid system (101x7x11) took less computation time but the error was more than 7%. Though, the other two grid systems (301x21x31 and 401x14x21) gave good results, the relative error being less than 5% but computation time was more than 20 hours and 30 hours, respectively. Hence, the 201x14x21 grid was selected as a typical grid and all other computations were carried out using this grid system.

Streamline distributions predicted from numerical simulations for 50 % wt glycerin and 70 % wt glycerin solutions with speed ratio of 1, 2 and 4 are shown in Fig. 6. At low speed ratio of 1, 'double eddy' structure was formed for 50% wt. glycerin solution. The two eddies were formed near the region of film splitting point. The thickness on the surfaces of two rolls was almost same. When speed ratio was

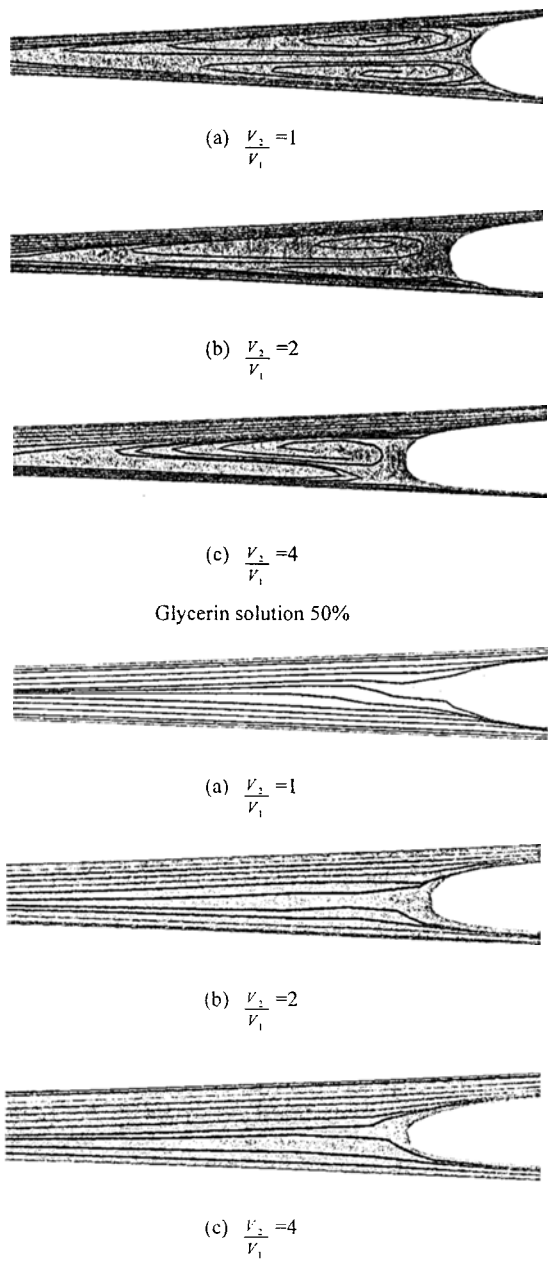

Fig. 6. Predicted streamline distributions for 50 % wt glycerin and 70 % wt glycerin solutions with speed ratio of 1, 2 and 4.

increased, the film started to split and caused eddies or recirculations to shrink. The upstream film thickness found increased while downstream film thickness decreased. For 70% wt. glycerin, no recirculation zones or eddies were present but the stream lines are straight parallel to the direction of the flow. As the speed ratio was increased, the film thickness on the applicator roll increased and the film thickness on pick-up roll decreased.

Variation of gauge pressure against the film splitting distance (x) from symmetric plane at nip point for 50 % wt glycerin and 70 % wt glycerin solutions with speed ratio of 1, 2 and 4 is shown in Fig. 7. In both cases, pressure reaches a peak value and suddenly decreases to a negative peak value and attains a near zero value. Since the fluid splitting takes place at the symmetry point, there is an abrupt change of pressure value from positive peak to a negative peak value.

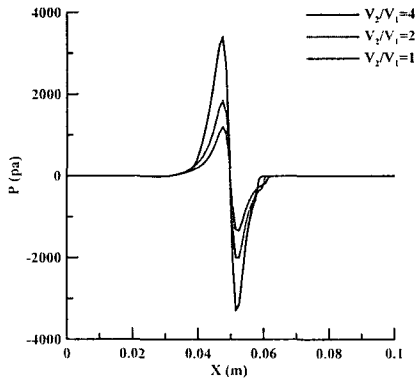

(a) 50% wt

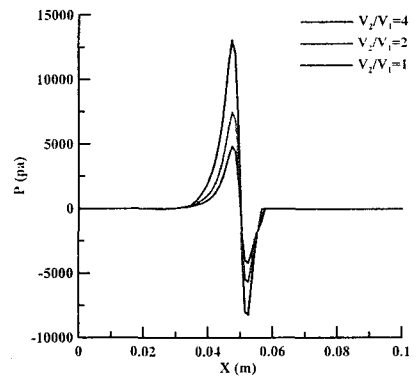

(b) 70% wt

Fig. 7. Gauge pressure distributions for 50 % wt glycerin and 70 % wt glycerin solutions with speed ratio of 1, 2 and 4.

The variation of the coating film thickness against speed ratio for both experimental and numerical results is shown in Fig. 8. Plots are shown for both 50% wt. glycerin and 70% glycerin solutions as coating fluid. The film thickness along the application roll or maximum film thickness values and film thickness along the pick-up roll or minimum film thickness values are compared with those obtained from the experiments. It is observed that maximum film thickness values are over-predicted by the numerical simulations and the error between two values within 5 to 10%. The reason may be due to the measurement error and other inherent errors existing during the coating process as it is very difficult to measure the exact coating film thickness even with sophisticated instrumentation.

Photographs of metered film coated on an applicator roll with 50% by weight glycerin solution and 70% by weight glycerin solution are shown in Figs. 9 and 10, respectively. Both rolls were rotated at 30m/min speed. It was observed that a uniform film

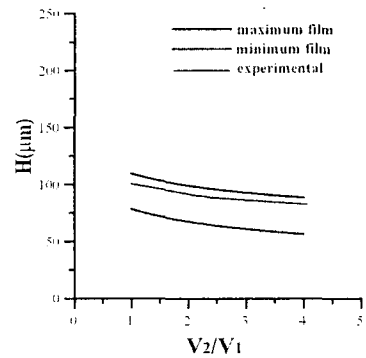

(a) Glycerin solution 50% wt

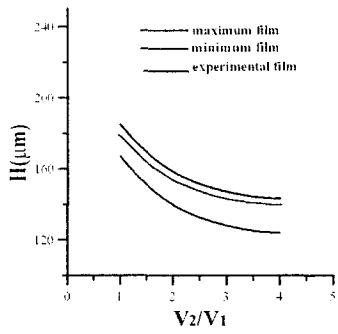

(b) Glycerin solution 70% wt

Fig. 8. Variation of coating film thickness with different speed ratios.

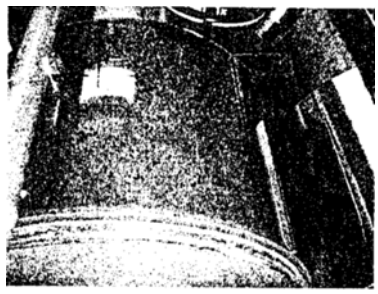

(a) Front view

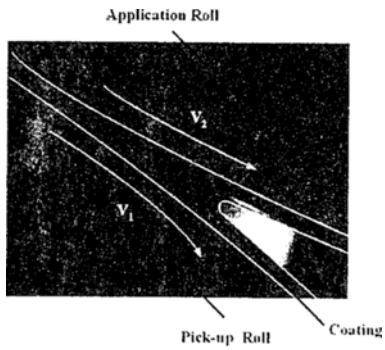

(b) Side view

Fig. 9. Metered film on the application roll for 50% wt glycerin solution with $v_1 = v_2 = 30$ m/min.

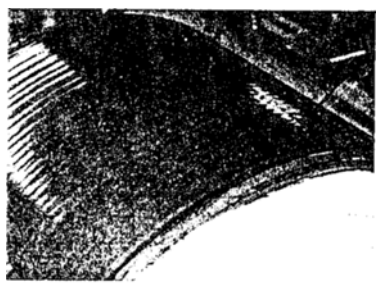

(a) Front view

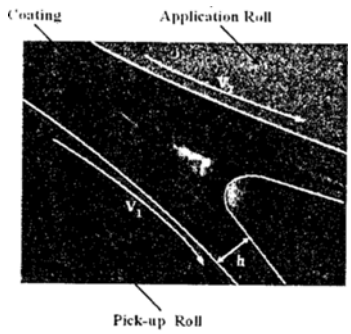

(b) Side view

Fig. 10. Metered film on the application roll for 70% wt glycerin solution with $v_1 = v_2 = 30$ m/min.

was produced for 50% glycerin solution at speeds $v_1 = v_2 = 30$m/min. On the other hand, the film produced with 70% glycerin solution was not uniform but it

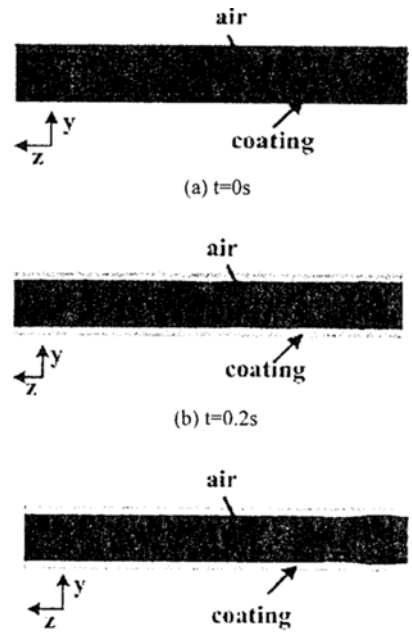

Fig. 11. Free surface profiles at x= 8 mm for 50% wt glycerin solution with $v_1 = v_2 = 30$ m/min.

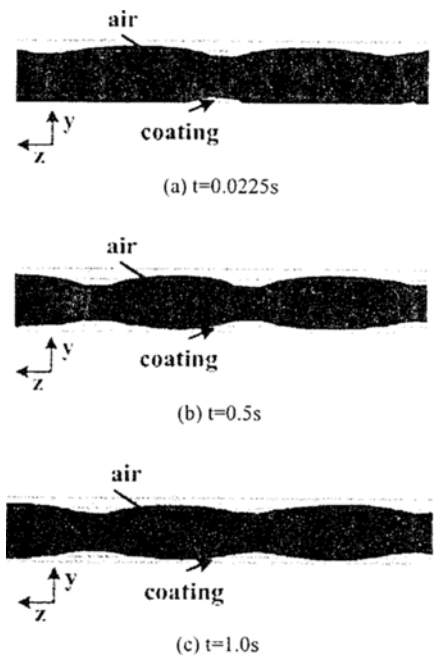

Fig. 12. Free surface profiles at x= 8 mm for 50 % wt glycerin solution with $v_1 = 30$ m/min and $v_2 = 120$m/min.

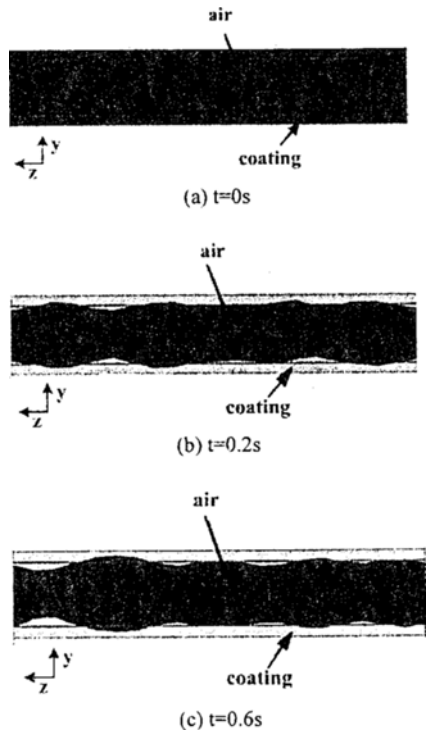

Fig. 13. Free surface profiles at x= 8 mm for 70% wt glycerin solution with v_1= v_2=30 m/min.

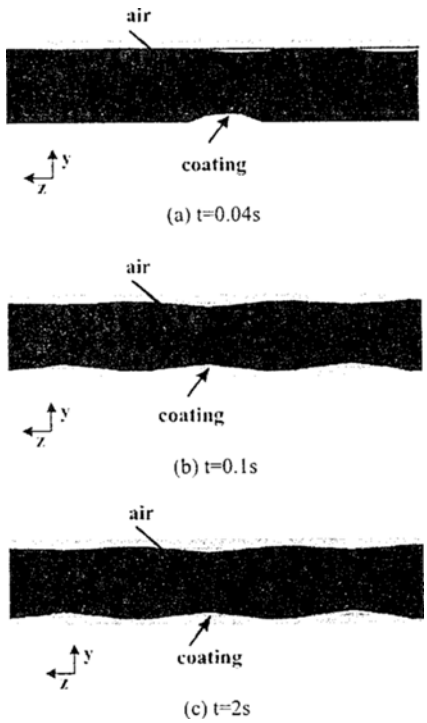

Fig. 14. Free surface profiles at x= 8 mm for 70 % wt glycerin solution with v_1= 30 m/min and v_2= 120m/min.

contained a wavy surface and hence the occurrence of ribbing. This is apparent from the fact that the viscosity of 70%wt glycerin solution is more than that for 50%wt glycerin solution.

Numerical results of free surface profiles at different time steps are shown in Figs. 11-14. Figures 11 and 12 are free surface profiles at x=8 mm for 50% wt. glycerin solution with speed ratio of 1 and 4 the pick-up roll speed being 30 m/min, respectively. For 50% wt glycerin solution with speed ratio 1, the coating film thickness was uniform and there was no significant effect of ribbing. Only a slight disturbance was observed in the uniformity of the coating film thickness at time t = 0.6 seconds. For a speed ratio of 4, the ribbing was observed at start of the coating process at time t =22.5 milliseconds. As the coating process continued, the ribbing phenomenon was significant and the wavelength of the ribbing increased rapidly.

Free surface profiles at x=8 mm for 70% wt. glycerin with speed ratio of 1 and 4 are shown in Figs. 13 and 14, respectively. The pick-up roll speed was 30m/min. For speed ratio 1, the ribbing occurred at the beginning of the coating process, but the smooth waviness was observed with little wave length. When the speed of the applicator roll increased to 120 m/min, the occurrence of the ribbing was predominant and non-uniformity in the coating thickness was very significant with large wavelengths of ribbing with high depths.

6. Conclusion

An effort has been made to analyze numerically and experimentally the three dimensional flow between two rolls of a forward roll coating process and to study the instability phenomena of ribbing. Experiments were conducted with aqueous glycerin solution as a coating fluid for two different glycerin concentrations of 50 % and 70%, the latter being more viscous than the former solution. Film thickness for different speed ratios of 1, 2 & 4 was measured by using an electronic micrometer needle. Experiments were carried out separately for each aqueous glycerin solution. The speed ratio is the most important factor which affects the coating film thickness. The ribbing occurs for 70% by wt. glycerin solution at speed ratio of 1, and the ribs with larger wavelength and depth are predominant for a speed ratio of 4. Results show that the distance from nip point to film splitting point

and the film thickness on the application roll increases with increase in speed ratio. But the film thickness on the pick-up roll decreases with the increase in speed ratio. Comparison of experimental results and numerical simulation results shows that the numerical computations over-predict the coating film thickness and error between the experimental results and numerical results being 5-10%. This error may be due to instrumental and other inherent errors during experiments. Thus, the numerical results give insight on the film thickness, the distance of film splitting point from nip point and also the speed at which ribbing occurs. Knowing these parameters prior to high volume production runs for forward roll coating enables industrial manufacturers to produce a uniform thickness of coating and the desired quality of the final product.

Acknowledgment

Authors acknowledge the financial and experimental support provided by China Steel Corporation, Kaohsiung, Taiwan.

Nomenclature

Ca : Capillary number
F : Volume fraction
H : Thickness of film, μm
H_0 : Roll gap, μm
N : Unit normal vector
P : Pressure, Pa
Pa : Ambient pressure, Pa
R : Radius of roller, mm
$\overline{\overline{T}}$: Tensor matrix in fluid
t : Unit tangential vector
v_1 : Pick-up roll speed, m/s
v_2 : Application roll speed, m/s
x, y, z : Cartesian coordinates

Greek symbols

μ : Viscous, kg/ m-s
ρ : Density, kg/m^3
σ : Surface tension, N/m
τ : Time, s

References

[1] D. J. Coyle, Knife and roll coating, S. F. Kistler and P. M. Schweizer, editors. Liquid Film coating. London, *Chapman & Hall, London.* (1997) 539-571.
[2] J. R. A. Pearson, The Instability of uniform viscous flow under rollers and spreaders, *J. Fluid Mechanics.* 7 (1959) 481-500.
[3] E. Pitts and J. Greiller, The flow of thin liquid films between rollers, *J. Fluid Mechanics.* 11 (1961) 33-50.
[4] C. C. Mill and G. R South, Formation of ribs on rotating rollers, *J. Fluid Mechanics.* 28 (1967) 523-529.
[5] J. Greener, T. Sullivan, B. Turner, S. Middleman, Ribbing instability of a two-roller coater, *Newtonian fluids. Chemical Engineering Communications.* 5 (1980) 73-83.
[6] M. Savage, Mathematical model for the onset of ribbing, *AICHE Journal.* 30 (1984) 999-1002.
[7] H. Benkreira, M. F. Edwards, W. Wilkinson, Ribbing instability in the roll coating of Newtonian fluids, *Plastic and Rubber Proc. Appl.* 2 (1982) 137-144.
[8] D. J. Coyle, C. W. Macoskoand, L. E. Scriven, Film-splitting flows in forward roll coating, *J. Fluid Mech.* 171 (1986) 183-207.
[9] D. J. Coyle, C. W. Macosko, L. E. Scriven, Stability of symmetrical film splitting between counter-rotating cylinders, *J. Fluid Mech.* 216 (1990) 437-458.
[10] T. Hasegawa, K. Sorimachi, Wavelength and depth of ribbing in roll coating and its elimination, *AICHE Journal.* 39 (1993) 935-945.
[11] M. E. Gurfinke, A. T. Patera, Three dimensional ribbing instability in symmetric forward roll film coating process, *J. Fluid Mechanics.* 335 (1997) 323-359.
[12] M. S. Carvalho, L. E. Scriven, Three-dimensional stability analysis of free surface flows: application to forward deformable roll coating, *Journal of Computational Physics.* 151 (1999) 534-562.
[13] C. W. Hirt and B. D. Nichols, Volume of fluid (VOF) method for the dynamics of free boundary, *Journal of Computational Physics.* 39 (1981) 201-225.
[14] CFD-ACE(U), CFD Research Corporation, Alabama, USA, (2003).